Journal of Volcanology and Geothermal Research xxx (2017) xxx–xxx

Contents lists available at ScienceDirect

Journal of Volcanology and Geothermal Research

journal homepage: www.elsevier.com/locate/jvolgeores

Storage conditions and magma processes triggering the 1818 CE Plinian eruption of Volcán de Colima

José Luis Macías [a,*], Giovanni Sosa-Ceballos [a], José Luis Arce [b], James E. Gardner [c], Ricardo Saucedo [d], Gabriel Valdez-Moreno [e]

[a] Instituto de Geofísica, Universidad Nacional Autónoma de México, Ex-Hacienda de San José de la Huerta # 8701, 58190 Morelia, Michoacán, Mexico
[b] Instituto de Geología, Universidad Nacional Autónoma de México, Coyoacán 04510, DF, Mexico
[c] Department of Geological Sciences, Jackson School of Geosciences, The University of Texas at Austin, Austin, TX 78712, USA
[d] Instituto de Geología, Universidad Autónoma de San Luis Potosí, Dr. M. Nava No 5, 78240 San Luis Potosí, Mexico
[e] Unidad Académica de Ciencias de la Tierra, Universidad Autónoma de Guerrero, Mexico.

ARTICLE INFO

Article history:
Received 1 December 2016
Received in revised form 15 February 2017
Accepted 26 February 2017
Available online xxxx

Keywords:
Amphibole xenocrysts
Hydrothermal experiments
Historic Plinian eruptions

ABSTRACT

Volcán de Colima has an eruptive history punctuated with explosive Plinian eruptions followed by long periods of effusive events. Both of the best documented Plinian eruptions, which occurred in 1818 CE and 1913 CE, emitted andesitic magma (~58 wt% SiO_2) that contains Pl > Opx > Cpx ≫ Amph + Fe-Ti oxides + Ap ± resorbed Ol, whereas effusive magmas from the 1819–1868 and 1962–2015 periods are particularly scarce in amphibole, and are slightly more silicic (59–61 wt% SiO_2). Pumice from the 1818 and 1913 deposits contain three groups of amphibole with different abundance, texture and composition. Composition is the most distinctive between them; the first group consists of crystals with high Al^{IV} (1.84–2.32), the second group of amphiboles is less abundant in Al^{IV} (1.45–1.76) and the third has low Al^{IV} (1.29–1.39). In contrast, amphibole from two Colima prehistoric lavas can only be grouped as medium Al^{IV} (1.45–1.76).

A set of hydrothermal experiments were carried out using a 1818 natural sample to investigate amphibole compositional variability with changes in pressure and temperature. Two groups of amphibole found in the Plinian deposits can be reproduced experimentally between 875 and 900 °C and 150–200 MPa. Another type of amphibole could not be equilibrated in the 1818 explosive Colima magma and their origin can be attributed to mixing with more mafic magmas. We found that amphibole abundance is greater in explosive events and that mafic inherited amphiboles can only be found in Colima Plinian deposits. When the influx of mafic magma is large or frequent enough, and they mix with more silicic Colima magma, then explosive events are more likely. If mafic melts cannot mix with the resident magmas or just pond and heat the reservoir, regardless of location in the plumbing system, then magmas can decompress more slowly and amphibole will have time to completely react out.

1. Introduction

For about a century, activity at Volcán de Colima, one of the most active volcanoes in North America, has been characterized by emission of lava flows and domes and their intermittent collapses that generate small pyroclastic density currents (Luhr and Carmichael, 1980; Medina-Martínez, 1983; De la Cruz-Reyna, 1993; Saucedo et al., 2005). In the past 24 years, however, eruptions have become increasingly more violent, prompting some scientists to claim that activity was tending towards a catastrophic eruption on the scale of the 1913 Plinian eruption (VEI = 4), which would threaten >300,000 inhabitants in the region (Saucedo et al., 2010). In fact, recent events in 2005 and 2015 have generated pyroclastic density currents (PDCs) with runouts of ~6 and 10.5-km from the crater, respectively (Macías et al., 2006; Capra et al., 2015), approaching the 15-km long PDCs produced during the 1913 Plinian eruption (Saucedo et al., 2005, 2010). The 1913 Plinian eruptions have served as the worst-case scenarios for constructions of hazard maps of the volcano (Saucedo et al., 2005; Capra et al., 2014). Despite the variation between mild lava emissions and explosive Plinian eruptions, most eruptions tap andesite with very similar mineralogy. The exception, however, is amphibole, a hydrous silicate mineral, which occurs in noticeably greater abundances in andesite erupted in 1818 and 1913 (Luhr, 2002; Saucedo et al., 2010; Savov et al., 2008). Because amphibole is rare in products from 1819 to 1868 and 1962–2015 periods (0–1 vol%), but relatively abundant in the explosive eruptions of 1818 and the 1869–1913 period (2.4–5.3 vol%) (Luhr, 2002;

* Corresponding author.
E-mail address: macias@geofisica.unam.mx (J.L. Macías).

http://dx.doi.org/10.1016/j.jvolgeores.2017.02.025
0377-0273/

Savov et al., 2008; Saucedo et al., 2010), the presence of amphibole has been proposed to be a mineralogical indicator for impending explosive activity (Luhr and Carmichael, 1990a). Importantly, the appearance of amphibole could herald an increased water content of the magma at depth (Rutherford and Devine, 2003), and that increased volatile content could ultimately lead to more explosive activity. Hence, the origin of amphiboles in the Colima explosive products is fundamental to understanding the eruptive dynamics of a volcano that has become more explosive in recent years.

Magma mixing and assimilation has been related to the generation of explosively erupted magmas and recent Colima magmas forming domes, lava flows, and pyroclastic density currents (Luhr and Carmichael, 1980; Robin et al., 1990; Valdez-Moreno et al., 2006; Reubi and Blundy, 2008; Savov et al., 2008). For the 1913 Plinian magma, Luhr and Carmichael (1980) observed that concentrations of compatible trace elements could not be produced solely by fractional crystallization, and that magma mixing or mingling was likely a relevant process. Savov et al. (2008) showed that Colima Holocene high-K explosive magmas represent mixtures between subalkaline and alkaline magmas and suggest that these mixing events would contribute to trigger Plinian eruptions. Crummy et al. (2014) concluded that pulses of K-rich alkaline mafic magmas (phlogopite-rich) periodically enter the CVC plumbing system on timescales of a few thousand years and may trigger Plinian explosive eruptions.

Assimilation of the local crust has been more controversial. Savov et al. (2008) argued that the basement plays no role in the composition of the post 1818 Volcan de Colima rocks whereas Reubi and Blundy (2008) concluded that high-K melt inclusions in plagioclase resulted from dissolution of higher-pressure (>200 MPa) amphibole, plagioclase, magnetite and biotite cumulates or plutonic rocks during assimilation in the ascending melt. Such plutonic rocks (microgabbro and granodiorites) were found as xenoliths in andesitic Colima lava flows (Valdez-Moreno et al., 2006). Based on Sr, Nd and O isotopes, the same authors suggest that assimilation of the local crust modified the composition of the Colima lavas.

The aim of this study is to investigate the mixing processes previously characterized in the 1818 and 1913 samples and to elucidate if such perturbations to the magmatic system describe the magmatic processes that have characterized the dynamics of explosive eruptions at Colima. Our investigation focuses on the origin of amphibole found in the 1818 and 1913 deposits and their relation with the explosive activity of the Colima volcano.

2. Geologic background

The Volcán de Colima is located in the western part of the Trans-Mexican Volcanic Belt (TMVB), a continental volcanic arc formed by the subduction of the Rivera and Cocos plates underneath the North America plate (Allan and Carmichael, 1984; Pardo and Suarez, 1995; Luhr, 1997) (Fig. 1A). This sector of the TMVB is characterized by a triple point junction formed by the Tepic-Zacoalco rift to the NW, the Chapala rift to the E, and the Colima graben to the S (Luhr et al., 1985; Garduño and Tibaldi, 1991) (Fig. 1B). The Volcán de Colima (19°30′45″; 103°37′; 3860 m above sea level) is located 30 km north of the City of Colima. It is the youngest volcano of the N-S volcanic chain formed by the Cántaro, Nevado de Colima and Volcán de Colima volcanoes known as the Colima Volcanic Complex (CVC) (Luhr and Carmichael, 1980).

Inception of the CVC volcanism began with the emission of lava flows followed by dacitic domes that formed the Cántaro stratovolcano between 1.7 and 1 Ma (Allan and Carmichael, 1984; Allan, 1986). Afterwards, the focus of volcanism migrated ~15 km to the south to establish Nevado de Colima volcano around 0.53 Ma (Mooser, 1961; Robin et al., 1987; Cortés et al., 2005, 2010). Nevado de Colima has had a very complex evolution, through the construction of volcanic edifices destroyed by central explosions or flank collapses (Robin et al., 1987; Cortés et al., 2010). This complex activity has not been precisely dated, although it apparently occurred from 0.53 to 0.03 Ma ending with the extrusion of andesitic lavas and El Picacho dome.

During late Pleistocene, volcanism again migrated to the south building the Paleofuego volcano (Robin et al., 1987). Paleofuego remains cover an area of ~70 km^2 and have a total estimated volume of 79 km^3 (Cortés et al., 2010). So far, the oldest sequence related to the activity of Paleofuego are pyroclastic flows, lahars and lacustrine deposits dated at 38,400 yr BP (Komorowski et al., 1994; Cortés et al., 2005) yielding a minimum age for its formation. This age suggests that Paleofuego was coevally active with the last stages of activity of Nevado de Colima. Paleofuego had a complex evolution with the construction and destruction of edifices by sector collapses producing multiple debris avalanche deposits (Robin et al., 1987; Luhr and Prestegaard, 1988; Komorowski et al., 1997; Cortés et al., 2010; Roverato et al., 2011; Roverato and Capra, 2014). The modern remains of Paleofuego are represented by 300 m thick walls made of andesitic lava flows alternated with block-and-ash flow deposits shaping a 5 km wide crater open to the south (Robin et al., 1987; Luhr and Prestegaard, 1988).

Sometime around 4 ka magmatism once again migrated to the south inside the remains of Paleofuego, building Volcán de Colima. This volcano has collapsed twice at 3060 yr BP (Cortés et al., 2010) and 2500 yr BP (Siebe et al., 1992; Komorowski et al., 1997; Cortés et al., 2010) generating debris avalanche deposits. Today, Volcán de Colima is composed of interlayered andesitic lava flows and pyroclastic deposits. The volcano occupies an area of 20 km^2 and has a total volume of 9 km^3 (Cortés et al., 2010). It has had at least 25 explosive eruptions since 1576 CE (Luhr and Carmichael, 1980; Medina-Martínez, 1983; De la Cruz-Reyna, 1993; Saucedo et al., 2005). During this historic activity Colima volcano has experienced at least three Plinian eruptions, in 1576, 1818, and 1913; 12 Soufriére-type eruptions (dome explosion events); and at least nine Merapi-type events (gravitational collapse of domes) (Saucedo et al., 2005). The eruptive history of Colima volcano shows that large magnitude eruptions occur every ~100 years, like those events from 1606, 1690, 1818, and the most recent in 1913 (Luhr and Carmichael, 1990b; Robin et al., 1991). The persistent activity of the volcano has made identification and description of deposits associated with large magnitude events difficult (Luhr and Carmichael, 1990b; Robin et al., 1991; Komorowski et al., 1994). Only the VEI = 4, 1913 Plinian eruption has been studied in detail (Saucedo et al., 2005, 2010) and has been used as a reference to discuss volcanic hazards and risk scenarios (Bonasia et al., 2011; Capra et al., 2014). In contrast, dominantly effusive periods that have taken place between explosive events have been better documented (Luhr and Carmichael, 1990b; Navarro-Ochoa et al., 2002). Most of these effusive products have been used to study the petrological, geochemical, and isotopic evolution of magmas (Luhr and Carmichael, 1980, 1990a; Verma and Luhr, 1993; Luhr, 2002; Mora et al., 2002; Valdez-Moreno et al., 2006; Savov et al., 2008; Saucedo et al., 2010; Reubi and Blundy, 2008; Reubi et al., 2013; Crummy et al., 2014).

2.1. The 1818 and 1913 deposits

The 1818 fallout deposits are exposed on the northern flanks of Volcán de Colima (Fig. 1C). These deposits usually cover a dark-brown paleosol that is a few centimeters thick (Fig. 2). From the base upward the 1818 deposits consists of a 1–3 cm thick fine ash bed (irregular thickness) with a basal erosive contact. This bed was emplaced by a dilute PDC. On top of this layer rests a massive tan clast-supported bed that varies in thickness from 7 cm at VC 01-06 to 27 cm at VC-11-06. It is composed of pumice (≤5.6 cm), and angular lithics (≤5.9 cm). Pumice is tan, angular and moderately vesicular and contains phenocrysts of plagioclase, pyroxene and amphibole. This bed was dispersed from a vertical eruptive column. Unfortunately, we do not have enough data to construct isopachs to portray

Please cite this article as: Macías, J.L., et al., Storage conditions and magma processes triggering the 1818CE Plinian eruption of Volcán de Colima, J. Volcanol. Geotherm. Res. (2017), http://dx.doi.org/10.1016/j.jvolgeores.2017.02.025

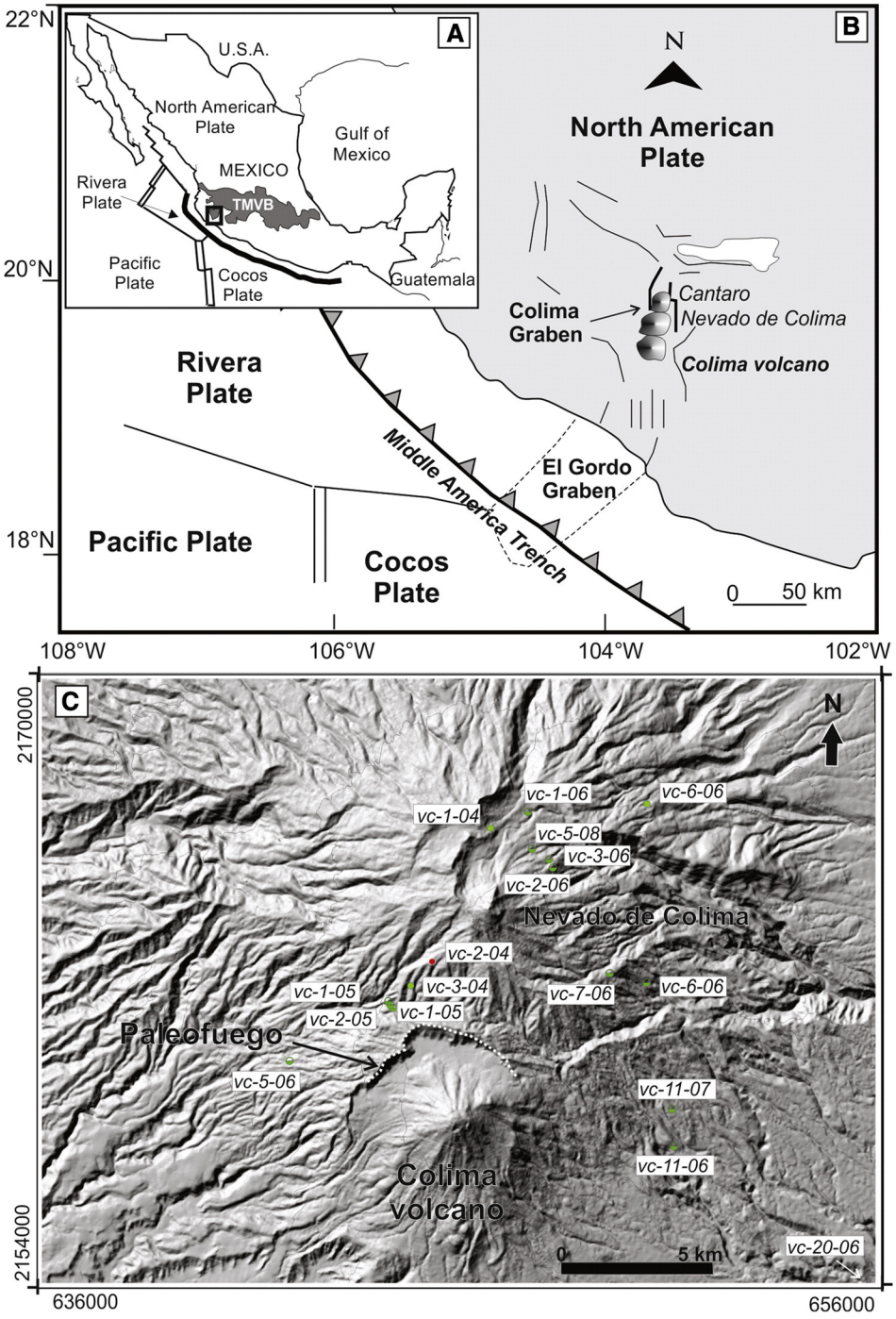

Fig. 1. A) Location of Volcán de Colima at the western most part of the Trans-Mexican Volcanic Belt, B) The volcano sits at the southern end of the N-S Colima Volcanic Complex (CVC) formed by the Cántaro, Nevado and Volcán de Colima. The CVC has been built during the past ~1 Ma within the Colima Graben, C) Location of the stratigraphic sections visited of the 1818 and 1913 deposits. Additional locations of the 1913 fallout deposit were published elsewhere (Saucedo et al., 2010).

the 1818 fallout dispersal because it has been widely eroded. This general stratigraphy preserved on the slopes of Nevado de Colima coincides with historic descriptions of the eruption. Waitz (1935) classified the 1818 eruption as a Peleean type because it began with the generation of "*nueé ardentes*" followed by the establishment of an eruptive column that was sustained during several hours, and reached an altitude of 15-km (Barcena, 1887; Arreola, 1915). These authors mentioned that the plume had an E-SE dispersal axis, with ash falling in Ciudad Guzman (25 km away where roofs collapsed) and in Mexico City (474 km E of the volcano). These descriptions were then summarized by several authors (Luhr and Carmichael, 1990b, Robin et al., 1990, Saucedo and Macías, 1999; Bretón et al., 2002). Recent descriptions of the mineral assemblages and the chemistry of pumice have been given by Savov et al. (2008) and Saucedo et al. (2010).

The 1913 fall deposit of Colima covers an area of ~191,000 km^2 with a volume of 0.56 km^3 (0.23 km^3 DRE = Dense Rock Equivalent) (Bonasia et al., 2011; Saucedo et al., 2011). Including the DRE volume of PDC deposits (0.07 km^3), the total DRE volume of the 1913 eruption is 0.30 km^3. The column height and volume suggests that the 1913 eruption had a VEI = 4 (Newhall and Self, 1982) being the largest in the historical record of Colima Volcano.

Please cite this article as: Macías, J.L., et al., Storage conditions and magma processes triggering the 1818CE Plinian eruption of Volcán de Colima, J. Volcanol. Geotherm. Res. (2017), http://dx.doi.org/10.1016/j.jvolgeores.2017.02.025

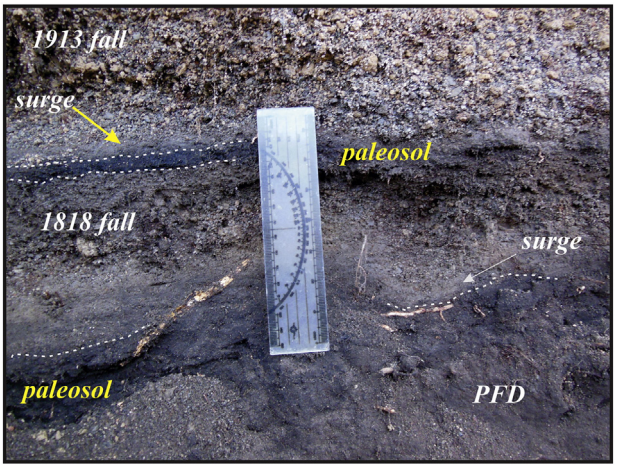

Fig. 2. Detailed view of the 1818 CE and 1913 CE tephra fall deposits of Volcán de Colima observed at section VC-2-04. These fallouts cover paleosols and discontinuous pyroclastic surge deposits rich in ash particles. Each fallout is rich in lapilli pumice.

According to Saucedo et al. (2010) the 1913 eruption occurred in three main phases (Opening, Vulcanian and Plinian) that produced small-volume PDCs which increase in size and volume through time. The last Plinian phase produced the fallout (C1 of Saucedo et al., 2010) and the longest PDCs known in the historical record of the volcano. In July 10–11, 2015, Colima generated 10.5-km long PDCs that are the second largest in historic times (Capra et al., 2015). The 1913 products of Colima have been described previously (Luhr and Carmichael, 1980; Robin et al., 1991) and consist of juvenile scoria and pumice with a mineral association of Pl > Opx > Cpx > Hbl + accessory titanomagnetite + Ap (Luhr and Carmichael, 1980; Robin et al., 1991; Savov et al., 2008; Saucedo et al., 2010) and rare Ol with reaction rims (Saucedo et al., 2010). Chemistry of juvenile scoria and pumice samples is andesitic as previously reported by several authors (Luhr and Carmichael, 1980, 1990a, b; Robin et al., 1991; Luhr, 2002; Valdez-Moreno et al., 2006; Savov et al., 2008; Saucedo et al., 2010) and very homogeneous as analyzed by Saucedo et al. (2010). Banded scoriae, olivine phenocrysts with reaction rims, and trace element variations support a magma mixing event shortly before the 1913 eruption (Saucedo et al., 2010).

2.2. Analytical methods

Major elements in plagioclase, clinopyroxene, orthopyroxene, amphibole, titomagnetite, illmenite, and groundmass glass were analyzed using a JEOL JXA-8600 electron microprobe (EPMA), housed in the Department of Geological Sciences at The University of Texas at Austin. Analyses were made using 15 keV accelerating voltage and 10 nA beam current. A focused beam was used to analyze plagioclase, pyroxenes, and the Fe-Ti oxides, but the beam was defocused to 5 μm to analyze amphibole and to 10 μm to analyze groundmass glass, in order to mitigate sodium migration (Devine et al., 1995). In addition, to better constrain the Na-loss a time-dependent correction was applied using the Probe for Windows software. Amphibole was also analyzed with a JEOL JXA-8900R electron microprobe housed in the Geophysics Institute at UNAM using the same analytical conditions.

Ten grams of a 1818 pumice clast (Section VC-2-04) were ground to fine powder (2.5 phi) lightly crushed for use in hydrothermal experiments. All experiments were water saturated (pressure = water pressure) and run in $Ag_{70}Pd_{30}$ capsules (2 or 5 mm in diameter) in cold-seal pressure vessels made of either Waspaloy or TZM metal. All experiments were water saturated and buffered close to the Ni-NiO buffer reaction. All experiments were run at pressures and temperatures that are above the solidus.

For those runs in Waspaloy pressure vessels, capsules were welded at one end and starting material and distilled water were added. Sufficient water was added to ensure that a separate fluid was present throughout the run. The capsule was then weighed, welded shut, heated on a hot plate, and weighed again to check for leaks and ensure that no water was lost during welding. To ensure that a fluid remained present throughout the run, the capsule is weighed after quenching. In addition, when the capsule is split open a slight hiss is heard if fluid is present. Finally, fluid saturated samples contain bubbles. Equilibrium is approached by using aliquots of previously run material, one of which had run at a higher temperature and the other at a lower temperature. The powders were placed in separate, 2-mm-diameter $Ag_{70}Pd_{30}$ capsules, which were left open and placed inside a 5-mm-diameter $Ag_{70}Pd_{30}$ capsule to ensure that both materials equilibrated at the same pressure and temperature. Oxygen fugacity was buffered near that of the Ni-NiO buffer reaction by using a Ni filler rod and water as the pressurizing medium (Geschwind and Rutherford, 1992; Gardner et al., 1995).

For experiments in TZM pressure vessels, 2-mm-diameter $Ag_{70}Pd_{30}$ capsules were welded at one end, the pumice powder was added, and the capsule was crimped shut. Another 2-mm-diameter $Ag_{70}Pd_{30}$ capsule was welded at one end and loaded with Ni metal and NiO powder and crimped. Both capsules were then placed inside a 5-mm-diameter $Ag_{70}Pd_{30}$ capsule that contained enough distilled water to both saturate the sample and facilitate the reaction between the buffer materials. The 5-mm capsule was welded shut and checked for leaks. The pressurizing medium in the TZM pressure vessels was argon, to which several bars of methane were added to maintain hydrogen fugacity during the experiment (Sisson and Grove, 1993). At the end of each run, the buffer and water were checked to ensure that both Ni metal and NiO powder were still present and that the experiment was water saturated. If one was absent, the sample was discarded. Mineral phases were considered stable if they occur as euhedral microlites.

2.3. Petrology of 1818 and 1913 rocks

Pumice samples of the 1818 and 1913 Colima Plinian eruptions were used for mineral and glass analyses. The modal analysis in pumice from 1818 deposits was obtained with 1000 point counts and is formed by plagioclase (12–17 vol%), orthopyroxene (2–7 vol%), clinopyroxene (1–4 vol%), amphibole (1–5 vol%), titanomagnetite (1 vol%) and olivine (0.1 vol%).

Pumice clasts from the 1818 and 1913 deposits are andesitic in composition. Pumice from the 1913 eruption contains bands formed by vesicular groundmass of gray and dark-brown color. Although the high vol% of microlites included in the groundmass makes impossible to analyze the composition of the glass, visible banding suggest the mixing of different melts. Macro-banded pumice is absent in the 1818 eruption, the groundmass contains less vol% of microlites than the 1913 pumice, and yields a dacitic composition for the glass (69–70.7 SiO_2 wt%; Table 1).

The 1913 eruption was Plinian but it was preceded by a magma mixing event, and thus the rocks from the eruption include scoria and pumice, mineral disequilibrium textures and trace element variability (Saucedo et al., 2010). Pumice from the 1818 eruption has never been related to magma mixing. However, the bulk compositional variability of its pumice (Luhr et al., 2010) could result from mixing of different batches of magma.

The following section describes compositional and textural features in crystal populations of plagioclase, pyroxene, Fe-Ti oxides and amphibole that can be attributed to mixed populations of crystals. We focus on amphibole crystals because of the role that this mineral could play in the generation of Colima explosive eruptions.

Please cite this article as: Macías, J.L., et al., Storage conditions and magma processes triggering the 1818CE Plinian eruption of Volcán de Colima, J. Volcanol. Geotherm. Res. (2017), http://dx.doi.org/10.1016/j.jvolgeores.2017.02.025

Table 1
Representative groundmass glass, plagioclase and pyroxene compositions of 1818 and 1913 Colima samples.

	SiO_2 (wt.%)	TiO_2 (wt.%)	Al_2O_3 (wt.%)	FeO (wt.%)	MnO (wt.%)	MgO (wt.%)	CaO (wt.%)	Na_2O (wt.%)	K_2O (wt.%)	Total (wt.%)	An content (mol%)	Mg#
1818												
groundmass	69.92	0.61	14.10	3.78	0.08	1.42	2.41	5.31	2.37	100	nc	nc
	69.07	0.69	14.98	3.50	0.05	0.76	2.89	5.65	2.40	100	nc	nc
	70.75	0.52	14.47	3.48	0.08	0.57	2.07	5.50	2.56	100	nc	nc
plagioclase	56.23	na	26.98	0.59	na	na	10.10	6.34	0.21	100.6	46	nc
	52.53	na	28.51	0.78	na	na	12.71	3.83	0.22	98.6	64	nc
	56.07	na	27.55	0.53	na	na	10.59	5.74	0.26	100.9	50	nc
orthopyroxene	53.87	0.22	0.67	14.92	0.44	28.15	1.33	0.02	0.00	99.6	nc	65
	52.33	0.32	1.17	18.78	0.59	24.25	1.53	0.02	0.00	99.0	nc	56
	54.52	0.16	1.99	12.45	0.29	30.36	1.41	0.01	0.00	101.2	nc	71
clinopyroxene	51.31	0.56	2.11	9.12	0.39	15.21	21.57	0.43	0.01	100.7	nc	63
	51.69	0.41	1.53	9.52	0.38	16.02	20.63	0.41	0.01	100.6	nc	63
	49.77	0.68	3.03	8.72	0.29	15.63	20.34	0.35	0.00	98.8	nc	64
1913												
plagioclase	55.39	na	27.83	0.49	na	na	10.74	6.06	0.17	100.8	49	nc
	48.06	na	32.89	0.58	na	na	17.23	2.94	0.05	101.8	76	nc
	51.24	na	30.95	0.52	na	na	14.27	4.67	0.11	101.9	62	nc
orthopyroxene	53.09	0.26	0.94	16.62	0.53	26.42	1.21	0.04	0.00	99.1	nc	61
	53.44	0.17	1.30	15.69	0.50	27.30	1.35	0.04	0.01	99.8	nc	64
	54.24	0.13	1.20	17.21	0.58	27.12	1.16	0.04	0.00	101.7	nc	61
clinopyroxene	49.28	0.69	3.55	8.52	0.32	15.11	21.78	0.51	0.01	99.8	nc	64
	51.72	0.45	1.83	8.40	0.37	15.85	21.65	0.45	0.00	100.7	nc	65
	50.34	0.68	3.32	8.72	0.27	15.72	21.49	0.44	0.01	101.0	nc	64

Groundmass glass normalized to 100% on an anhydrous-basis. na = not analyzed; nc = not calculated.

2.4. Plagioclase

Plagioclase phenocrysts (100–800 μm in size) of both Plinian eruptions vary in composition between An_{40}-An_{80}; cores can be either sodium-rich or calcium-rich. Crystals in 1913 pumice are more calcic than crystals from 1818 (Supplementary material Table 1). Overall, plagioclase rims can be clustered into two groups. The first consists of rims with composition of $An_{60 \pm 2}$. The second group consists of rims with composition of $An_{50 \pm 2}$. Plagioclase with composition of An_{70} form inner zones and never forms the rim of crystals. Plagioclase is complexly zoned and two main textural populations can be identified: 1) phenocrysts with oscillatory zoning from core to rim, and 2) phenocrysts with sieved cores mantled by thick rims that can be hundreds of microns wide (Fig. 3A–C). Core-to-rim profiles show variations of up to 15 mol% of An content, but in general plagioclase is more calcic in zones close to the rim and in the zones that mantle the sieved cores (Fig. 3A–C).

2.5. Pyroxene

Orthopyroxene is more abundant than clinopyroxene in both the 1818 and 1913 magmas. Both reach 0.4 cm in size across the *c* axis, but most are smaller than 0.2 cm. Sieve textures are present in the cores of some orthopyroxene, but never close to the rim. Orthopyroxene and clinopyroxene compositions are diverse (Supplementary material Table 2), but generally cluster in two groups (Fig. 4). One group has a narrow Mg# range (55–65) (Mg# = Mg / (Mg + Fe_{total}) + 100) but different Al_2O_3 contents (0.6–4.5 wt%). A less abundant group of pyroxenes is more magnesian (Mg# = 70–80) with variable amounts of Al_2O_3 (1–4.5 wt%). Pumice from the 1818 and 1913 deposits contain both groups of pyroxenes.

2.6. Fe-Ti oxides

Titanomagnetite is the main Fe-Ti oxide in the 1818 and 1913 magmas, very few ilmenite crystals were found (Supplementary material Table 3). Ilmenite-titanomagnetite pairs in touch were not found. Mineral concentrates of titanomagnetite are not in equilibrium with the few ilmenite crystals found, as tested from their Mn/Mg distribution (Bacon and Hirschmann 1988). The scarce amount of ilmenite and the lack of equilibrium between these few ilmenites and titanomagnetites prevent calculations of pre-eruptive temperatures and fO_2 with the ilmenite-titanomagnetite geothermometer.

2.7. Amphibole

Amphibole in 1818 and 1913 magmas has variable sizes, abundances, compositions, and textures. In the 1913 rocks, crystals are more abundant and larger (0.5–1 cm across the *c* axis) than in the 1818 rocks where they can reach 0.07–0.5 cm across the *c* axis (Fig. 5a–d). Amphibole in both magmas varies significantly in composition (Table 2). Although generally pargasitic, amphibole compositions can be grouped into three categories (Fig. 6). The first Group (G1) consists of crystals with very high Al^{IV} (1.84–2.32). The second group of amphiboles (G2) consists of medium Al^{IV} (1.45–1.76) and the third (G3) has low Al^{IV} (1.29–1.39). The G1 crystals show a distinctive optical birefringence characteristic of high Fe or Mg contents. G1 amphiboles are more abundant (80%) in the 1913 pumice, whereas G2 amphiboles are more abundant (80%) in the 1818 samples. G3 amphiboles only occur in the 1818 pumice.

Reaction rims developed at the expense of amphibole in contact with the melt. Some of the largest crystals in the 1913 magma have thin rims (<2 μm) that consist of glass and microlites of pyroxene (Fig. 5a). All other amphiboles in the 1913 magma either lack reaction rims or contain rounded borders. Amphibole in the 1818 magma presents two types of reaction rims. The first type (TI) is more abundant, and consists of thin (<10 μm), black rims that are mostly too fined-grained to be resolved optically; a few were coarse enough to enable opaque phases, pyroxenes and glass to be identified (Fig. 5b). The second type (TII) (<2 vol%) consists of thick rims (10–15 μm) formed by microphenocrysts of pyroxene, plagioclase, opaques and glass (Fig. 5c). Overall, amphibole lack internal sieve textures, although some glass inclusions could occur.

We performed a series of hydrothermal experiments to investigate how amphibole change composition with pressure and temperature

Please cite this article as: Macías, J.L., et al., Storage conditions and magma processes triggering the 1818CE Plinian eruption of Volcán de Colima, J. Volcanol. Geotherm. Res. (2017), http://dx.doi.org/10.1016/j.jvolgeores.2017.02.025

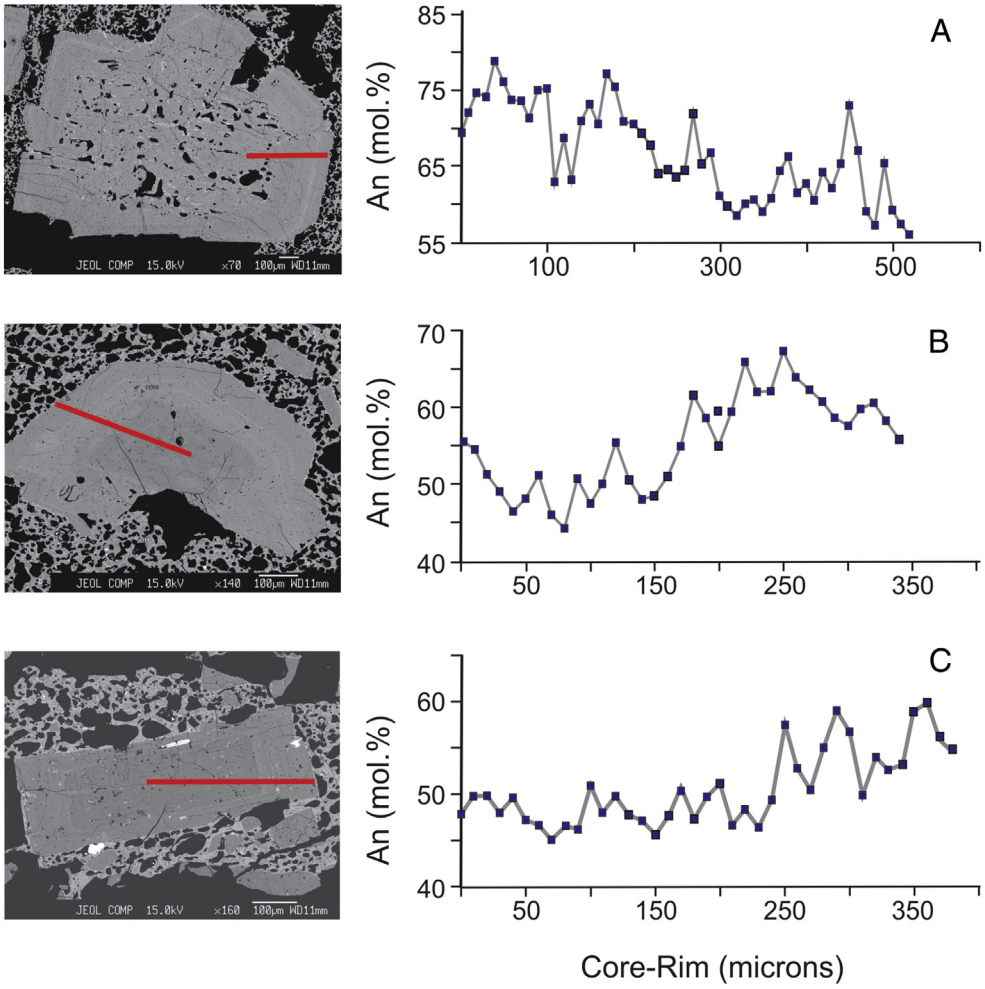

Fig. 3. Compositional transects and backscattered images of representative plagioclases from 1913 (A and B) and 1818 (C) deposits. Solid line across plagioclase represents the length and location of the analyzed transect. Solid bar on bottom of images represent a 100 μm scale bar. Note how regardless of the initial composition of the core, crystals recorded multiple increases of An-content produced by mixing-heating events and how zones close to the rims tend to be more An-rich.

and verify which of the group of amphiboles grew in the magma that produced the Plinian eruptions of Colima volcano.

3. Experimental results

Experiments were carried out using a 1818 whole-rock sample. The modal analysis of the pumice used for the experiments contains plagioclase (17 vol%) orthopyroxene (3 vol%), clinopyroxene (2 vol%), amphibole (1 vol%) and titanomagnetite (<1 vol%). Pumice fragments were lightly crushed to avoid the exposure of phenocryst cores into the experimental charges. This procedure was chosen as an attempt to adjust the composition of the reactive magma in the experiments (Pichavant et al., 2007). Indeed, the interpretation of phase equilibrium experiments in mixed magma systems can be difficult. Pichavant et al. (2007) showed that, with the procedure above (i.e., relatively coarse-grained pumice as starting material), partial equilibrium between melt and crystals can be attained after durations of a few days. In this work, we used newly grown phases (euhedral experimental amphiboles perpendicular to the c axis and euhedral experimental plagioclases) as partial equilibrium compositions, rather than rim compositions of phenocrysts which can be difficult to define (see Pichavant et al., 2007, their Fig. 7). In comparison, newly grown experimental phases were relatively easy to find in our experimental charges and their compositions could be related with the imposed T-P experimental conditions.

In order to approach the natural equilibrium state, we designed experiments that closely match previously reported P-T conditions for Colima magmas (discussed later). All experiments were run at pressures and temperatures where melt and fluid (bubbles) were present (Table 3). In all experiments Fe-Ti oxides and pyroxenes grew. At 100 MPa, amphibole and plagioclase are stable below ~960 °C (Fig. 7). At 150 MPa, amphibole crystallizes below 960 °C and plagioclase below ~950 °C (Fig. 7).

In general, lower temperature and lower pressure resulted in more silicic melts that are enriched in K_2O and depleted in FeO, MgO, and CaO. Plagioclase also varies in composition with pressure and temperature and, in general, becomes more albitic with decreasing temperature and decreasing pressure (Fig. 7). Overall, experimental amphibole becomes richer in Al_2O_3, MgO, and CaO as pressure increases at constant temperature; at constant pressure, amphibole also becomes more Al_2O_3-rich when temperature increases.

4. Discussion

Disequilibrium textures in phenocrysts and compositional variability in minerals and groundmass confirm that the 1818 and 1913 magmas were replenished with more mafic melts before eruption. Although the less evolved composition of the 1913 whole rocks compared to melt inclusions (Fig. 8) suggests that mixing with more mafic magmas occurred shortly before eruption, repeated mixing episodes are recorded in the 1818 and 1913 phenocrysts (Fig. 3).

Please cite this article as: Macías, J.L., et al., Storage conditions and magma processes triggering the 1818CE Plinian eruption of Volcán de Colima, J. Volcanol. Geotherm. Res. (2017), http://dx.doi.org/10.1016/j.jvolgeores.2017.02.025

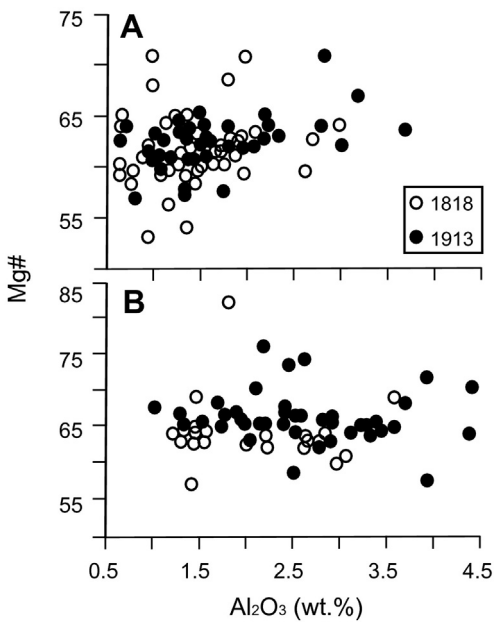

Fig. 4. Compositional variation of orthopyroxenes (a) and clinopyroxenes (b) from the 1818 (open symbols) and 1913 (solid symbols) Colima Plinian eruptions. Orthopyroxene and clinopyroxene display the full range of Al_2O_3 contents, but can be separated into two groups as a function of Mg#. For details on compositional groups of pyroxenes see the text.

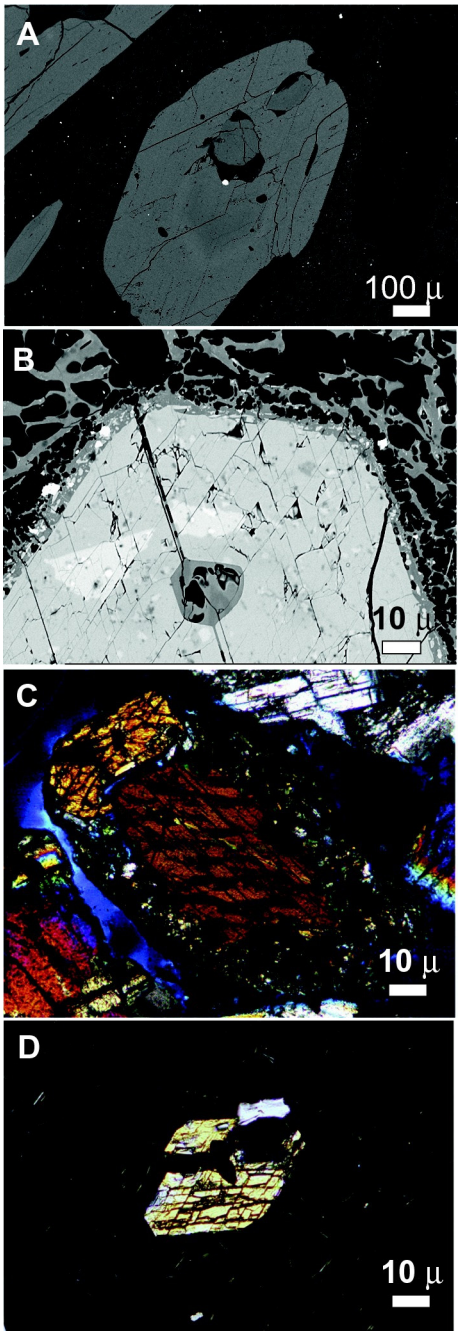

Fig. 5. Backscattered images (a–b) and polarized light microphotographs (c–d) of 1818 and 1913 amphiboles. a) phenocryst with rounded corners in 1913 magma, b) TI rim in 1818 amphibole, c) TII rim in 1818 amphibole, and d) microphenocrysts in 1818 magma.

The mixed nature of the 1818 and 1913 Colima rocks makes calculations of pre-eruptive intensive parameters challenging. The absence of Fe-Ti oxide pairs in equilibrium in the 1818–1913 rocks precludes the calculation of pre-eruptive temperature. Compositions of coexisting pyroxenes in the 1913 eruption products yield temperature estimates of ~900 to 985 °C (Luhr, 1992, 2002). More recently, Savov et al. (2008) proposed temperatures <950 °C based on the andesitic melt composition of the 1913 magma and the presence of amphibole. In order to better constrain the experimental temperature, we calculated crystallization temperatures with plagioclase rims and G3 and G2 amphiboles (Holland and Blundy, 1994). Temperatures were calculated either with the quartz saturated or the quartz absent models. If we assume that the low ^{IV}Al amphibole (G3) and the An_{50} rims are in equilibrium in the magma, then the equilibrium temperature would have been 880 °C ± 20. If we assume that the G2 amphiboles were in equilibrium with the An_{60} rims, the equilibrium temperature would have been 910 °C ± 20.

As with temperature, the pre-eruptive pressure has not been well constrained. Previous studies found 3.4–6.2 wt% of water dissolved in orthopyroxene melt inclusions from the 1913 magma (Atlas et al., 2006; Luhr et al., 2006) implying pressures of 90–200 MPa for andesitic magmas (Papale et al., 2006). However, it is unclear if the analyzed melt inclusions come from either xenocrysts or phenocrysts and, so, these pre-eruptive pressures are uncertain. Glass in our experiments yield insight about the pre-eruptive pressure of the 1818 Colima magma. We used an average temperature of 895 °C ± 20 as calculated with the amphibole-plagioclase geothermometer. In order to match this temperature range and the natural glass composition, experimental glasses should be equilibrated at 207 ± 52 MPa (Fig. 9). Alternatively, we used the hygrometer proposed by Waters and Lange (2015). According to the model, the bulk composition of the 1818 magma should yield plagioclase with An_{55} composition at 895 °C ± 20 and water contents of 5.3–61 wt%. Such water contents would saturate at pressures of 170–210 MPa (Papale et al., 2006). The pressure required to equilibrate experimental glasses at 895 °C ± 20 overlap the pressure calculated with the hygrometer (170–210 MPa), and as shown below, this temperature-pressure range match well the conditions at which G2 and G3 amphiboles could have been equilibrated.

In addition to constraints on pre-eruptive pressure, our experiments were performed to investigate if the compositional variability in the 1818 and 1913 amphiboles could be related with temperature-pressure variations and if such variations could represent melts with variable composition. Amphibole crystallized in both melting and crystallization experiments. The composition of the experimental amphibole shows the effect of imposed changes in temperature and pressure on a hybrid melt. Previous studies have shown that two samples with the same bulk composition but one sample containing xenocrysts and the other sample in equilibrium, yield experimental amphibole with similar composition at a given pressure and temperature (Sosa-Ceballos et al., 2014). When experimental amphiboles are compared to natural compositions

Please cite this article as: Macías, J.L., et al., Storage conditions and magma processes triggering the 1818CE Plinian eruption of Volcán de Colima, J. Volcanol. Geotherm. Res. (2017), http://dx.doi.org/10.1016/j.jvolgeores.2017.02.025

Table 2
Chemical analyses of amphibole in samples of the 1818–1913 eruptions, prehistoric lavas (LHV, BSA), xenoliths, and experiments.

Eruption	SiO_2 (wt%)	TiO_2 (wt%)	Al_2O_3 (wt%)	FeO (wt%)	MnO (wt%)	MgO (wt%)	CaO (wt%)	Na_2O (wt%)	K_2O (wt%)	Total (wt%)	Al IV
1818	43.51	2.71	9.86	12.67	0.25	13.49	10.96	2.22	0.45	96.13	1.49
	43.07	1.83	10.56	12.79	0.22	13.58	11.01	2.18	0.37	95.63	1.52
	41.80	2.56	10.58	12.80	0.27	12.99	11.07	2.15	0.42	94.68	1.62
	42.19	3.26	10.50	11.33	0.15	13.47	11.10	2.31	0.52	94.84	1.61
	44.44	2.46	12.63	10.14	0.12	15.12	11.28	2.49	0.57	99.25	1.65
	44.20	2.95	11.13	12.47	0.19	14.06	11.15	2.30	0.44	98.89	1.59
	44.77	2.95	10.68	12.21	0.17	14.25	11.15	2.42	0.44	99.05	1.52
	44.34	2.44	11.18	12.84	0.21	13.98	10.98	2.39	0.40	98.77	1.55
	44.32	2.52	10.99	13.90	0.18	13.53	11.10	2.30	0.47	99.34	1.56
	44.81	2.96	10.54	12.76	0.20	14.06	11.10	2.42	0.45	99.33	1.52
	45.51	1.78	9.92	12.88	0.27	14.63	11.02	2.20	0.39	98.62	1.38
	45.15	2.19	9.81	12.17	0.26	14.48	10.98	2.17	0.39	97.58	1.39
	44.67	2.54	10.69	13.02	0.23	14.06	11.03	2.29	0.43	99.03	1.51
	44.01	2.48	11.30	12.66	0.16	14.06	11.16	2.42	0.38	98.67	1.59
	44.66	2.34	10.58	12.15	0.21	14.09	10.99	2.28	0.45	97.76	1.46
	44.99	2.81	10.43	12.83	0.21	13.72	10.92	2.40	0.47	98.78	1.46
	43.69	2.52	11.93	10.85	0.18	14.40	11.13	2.32	0.36	97.44	1.61
	46.26	2.03	9.74	12.13	0.30	14.52	10.84	1.99	0.40	98.25	1.29
	39.03	2.74	11.99	11.63	0.22	16.01	11.46	2.46	0.37	95.91	2.10
	38.95	2.87	11.93	11.62	0.15	14.90	11.30	2.35	0.35	94.42	2.03
	37.93	2.32	13.03	11.06	0.16	15.94	11.56	2.41	0.33	94.74	2.20
	37.41	2.94	11.96	11.69	0.19	15.39	11.42	2.40	0.35	93.74	2.19
	41.37	2.06	12.99	9.75	0.21	16.63	11.73	2.41	0.27	97.42	1.94
	41.60	2.08	13.87	10.88	0.18	16.55	11.84	2.39	0.31	99.70	2.02
	39.25	2.72	12.82	12.71	0.18	15.32	11.51	2.45	0.36	97.31	2.13
	41.63	2.93	12.26	12.65	0.21	15.41	11.68	2.44	0.37	99.59	1.95
1913	43.76	2.99	11.43	12.67	0.17	13.57	11.10	2.32	0.52	98.54	1.62
	43.82	2.75	11.40	12.42	0.21	13.86	11.11	2.38	0.49	98.48	1.61
	44.62	2.09	10.92	12.12	0.18	14.47	11.25	2.28	0.43	98.37	1.51
	43.72	3.10	11.15	12.80	0.18	13.83	11.23	2.56	0.50	99.10	1.64
	43.66	3.02	11.06	12.70	0.16	13.89	11.13	2.40	0.43	98.46	1.62
	44.64	2.95	10.36	12.26	0.16	14.28	11.07	2.42	0.40	98.58	1.51
	42.98	2.81	11.73	12.55	0.20	13.74	11.10	2.44	0.42	97.98	1.69
	42.74	2.95	10.78	12.52	0.20	13.75	11.09	2.31	0.39	96.73	1.64
	43.77	2.88	12.11	10.99	0.16	14.66	10.94	2.69	0.44	98.67	1.67
	44.14	3.10	11.41	12.11	0.21	14.04	11.04	2.31	0.43	98.82	1.60
	44.77	2.90	11.22	10.79	0.14	15.08	10.57	2.48	0.37	98.38	1.54
	44.23	3.15	11.26	11.95	0.14	13.94	11.11	2.37	0.41	98.56	1.58
	43.32	2.31	11.99	12.45	0.18	13.87	11.10	2.50	0.47	98.23	1.66
1913	42.60	2.62	10.91	12.83	0.20	13.35	11.00	2.37	0.51	96.41	1.62
	42.81	3.17	11.11	12.37	0.16	14.00	11.20	2.49	0.45	97.78	1.69
	41.50	3.11	11.26	12.74	0.14	13.53	10.98	2.47	0.52	96.30	1.76
	44.18	2.76	11.28	12.43	0.17	13.90	11.06	2.47	0.49	98.72	1.58
	44.14	3.13	11.06	12.09	0.17	14.17	11.18	2.48	0.48	98.90	1.60
	44.33	2.60	11.15	13.04	0.21	13.88	10.96	2.41	0.49	99.10	1.57
	44.03	2.91	11.38	12.79	0.22	13.83	11.02	2.47	0.51	99.16	1.61
	36.89	2.69	13.11	12.80	0.20	15.36	11.18	2.50	0.41	95.14	2.32
	37.74	2.33	12.46	12.96	0.30	14.79	11.31	2.47	0.38	94.73	2.17
	42.96	2.40	12.68	12.10	0.12	15.48	11.76	2.52	0.39	100.40	1.85
	42.96	3.13	12.21	12.58	0.19	15.26	11.67	2.54	0.46	100.99	1.86
	39.43	3.54	13.36	11.99	0.17	15.44	11.67	2.58	0.45	98.62	2.20
	38.68	3.26	13.53	12.13	0.13	15.42	11.54	2.73	0.35	97.77	2.25
LHV	43.43	1.74	10.33	12.51	0.18	14.25	10.88	2.16	0.29	96.14	1.49
	43.16	1.74	11.01	12.30	0.19	14.12	10.84	2.08	0.33	96.18	1.54
	42.91	2.10	10.97	12.67	0.20	13.88	10.85	2.14	0.31	96.40	1.58
	42.81	2.10	10.93	12.77	0.20	13.75	10.88	2.27	0.28	96.38	1.58
	42.42	2.86	10.03	13.31	0.38	13.46	10.54	2.27	0.29	95.95	1.58
	42.15	2.73	10.22	13.43	0.29	13.45	10.74	2.36	0.34	96.13	1.62
	42.25	2.33	11.50	11.12	0.13	14.28	10.90	2.34	0.33	95.51	1.66
	42.04	1.99	10.91	12.78	0.15	13.91	10.76	2.28	0.34	95.48	1.63
	42.19	1.93	11.20	10.04	0.08	15.35	11.05	2.26	0.30	94.72	1.64
	43.32	2.62	11.04	12.67	0.16	13.71	10.81	2.38	0.36	97.41	1.59
	43.71	1.74	11.86	9.56	0.13	15.53	11.03	2.28	0.31	96.55	1.58
BSA	44.34	2.45	10.14	12.71	0.20	13.94	10.73	2.01	0.40	97.33	1.44
	43.76	2.34	11.26	11.96	0.13	13.92	10.95	2.26	0.35	97.22	1.55
	43.10	2.00	12.38	10.90	0.16	14.84	10.99	2.40	0.36	97.44	1.68
	42.76	2.41	11.68	12.39	0.13	14.11	10.90	2.41	0.38	97.50	1.68
	41.01	1.86	11.77	10.63	0.16	14.80	10.86	2.19	0.32	94.02	1.74
	40.86	2.26	11.00	11.81	0.12	14.17	10.67	2.35	0.35	93.93	1.72
	42.63	2.78	11.59	12.14	0.12	13.69	10.85	2.37	0.41	96.93	1.66
	42.66	2.76	11.34	11.85	0.16	13.97	10.98	2.31	0.39	96.81	1.65
Exp 9	42.38	2.52	11.08	12.27	0.19	14.21	11.29	2.98	0.31	97.24	1.71
Exp 10	48.41	0.75	6.30	9.03	0.31	17.39	11.37	1.87	0.23	95.66	1.72
Exp 16	42.35	2.03	9.52	12.42	0.24	14.33	11.16	2.70	0.31	95.05	1.54

Please cite this article as: Macías, J.L., et al., Storage conditions and magma processes triggering the 1818CE Plinian eruption of Volcán de Colima, J. Volcanol. Geotherm. Res. (2017), http://dx.doi.org/10.1016/j.jvolgeores.2017.02.025

Table 2 (*continued*)

Eruption	SiO_2 (wt%)	TiO_2 (wt%)	Al_2O_3 (wt%)	FeO (wt%)	MnO (wt%)	MgO (wt%)	CaO (wt%)	Na_2O (wt%)	K_2O (wt%)	Total (wt%)	Al IV
Exp 24	48.11	0.96	7.56	8.86	0.39	17.42	11.35	1.86	0.29	96.81	1.04
Exp 30	45.34	2.30	9.12	11.68	0.35	13.67	10.58	2.55	0.40	96.00	1.26
Xenolith	40.28	3.51	12.05	11.77	0.57	13.47	10.64	2.83	0.40	95.51	1.90
	40.80	3.44	12.05	12.07	0.58	13.46	10.55	2.71	0.47	96.12	1.86
	41.92	3.29	11.61	12.08	0.65	13.76	10.64	2.52	0.49	96.95	1.76
	42.19	3.37	11.97	12.57	0.76	13.70	10.72	2.61	0.49	98.38	1.80
	41.99	2.38	12.56	11.62	0.61	14.14	10.75	2.42	0.39	96.86	1.78

Amphibole on experiments represents an average of 5 analyses.
FeO = Fe total.
AL IV = number of Al atoms in tetrahedral site.

(Fig. 6), it is clear that G1 amphiboles would have equilibrated in a more mafic melt than G2 and G3, and at higher pressure as shown by its low totals-higher water content (Table 2). In fact, amphibole with similar composition to G1 crystals found in Mount Pelée has been demonstrated to be in equilibrium with more mafic melts (Pichavant et al., 2002). Recent investigations have suggest the existence of a low velocity zone 15 km below the Colima volcano where mafic magma accumulates in a swarm of dykes (Spica et al., 2016). Such a zone could be the reservoir where G1 amphiboles equilibrate and then ascend with mafic volatile-rich melts to shallower chambers. G2 and G3 amphiboles can be reproduced experimentally in the ~890 °C and 170–210 MPa temperature-pressure field (Fig. 6). G3 crystals have low relative abundance and contain euhedral faces so their origin could be attributed to growth of new crystals in the hybrid magma produced by the mixing event (e.g. Coombs et al., 2002; De Angelis et al., 2013). Given the nearly equivalent bulk composition of the 1913–1818 magmas we propose that the G1 amphiboles did not equilibrate in the Colima Plinian magmas and that they must have been added to the Colima reservoir by a mixing or assimilation process.

4.1. Magma processes during Plinian events at Volcán de Colima

The occurrence of xenocrysts in the Colima deposits suggests that assimilation and/or mixing modify the Colima magmas. Amphibole in xenoliths found in Colima prehistoric lavas have distinctive composition (Fig. 6) and we did not find them included in the lava. Thus it is unlikely that amphibole xenocrysts were incorporated from assimilate of the

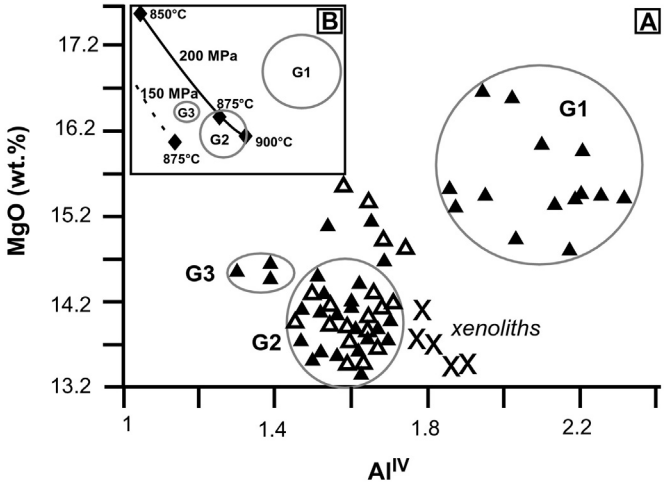

Fig. 6. Compositional variations of amphiboles in natural samples,G1, G2 and G3, (filled circles), amphibole grown in experiments at 150–200 MPa and 825–900 °C (filled rhombs), prehistoric lavas, LHV and BSA, (empty circles) and amphiboles from xenoliths included in BSA (empty triangles). The solid line represents a 200 MPa experimental isobar. Dashed lines represent inferred isobars at 150 MPa. Most of G2 amphiboles cluster between 150 and 200 MPa isobars and should crystallized at temperatures between 875 and 900 °C.

local crust. We analyzed amphibole in two prehistoric lavas, Los hijos del volcán (LHV) and lavas from Barranca de San Antonio (BSA), a xenolith-hosting lava, (Valdez-Moreno et al., 2006) and their composition and texture match those of the G2, never G1, amphiboles found in the Plinian deposits (Fig. 6).

Amphibole in the 1818 and 1913 andesites can be found in equilibrium with the surrounding matrix, with rounded margins, or surrounded by either a thin black rim (TI), or a thick well crystallized reaction rim (TII). Given the explosive nature of 1818 and 1913 deposits, we interpret all reaction rims (TI and TII) to record breakdown from heating and mixing (Rutherford and Devine, 2003; Chertkoff and Gardner, 2004). Amphibole phenocrysts in equilibrium with the surrounding matrix are scarce, whereas amphiboles with TI rims are the most abundant. Only a few amphiboles (>1% in any sample) present TII rims. Pyroxene crystals in the rim can be explained by a rise in magma temperature above 975 °C at 200 MPa where amphibole is not stable. Although most unrimmed amphiboles have straight borders, some crystals have rounded edges suggesting an episode of resorption where eruption occurred before rims could develop.

Amphiboles in BSA and LHV prehistoric lavas contain only TII rims, although thinner than the Plinian amphiboles. Given the effusive nature of these samples, the rims could reflect either slow decompression rates, heating, or a combination of these processes (De Angelis et al., 2013). Ongoing investigations will determine the origin of amphiboles in the Colima lavas, including some 2015 events.

Compositional and experimental evidence also demonstrate the active role of mixing in the Colima magmatic system to trigger Plinian eruptions. The outer ~An_{60} rims (Fig. 3) on the plagioclase phenocrysts and the few Mg-rich pyroxenes may be associated with the last heating event that affects the Colima magma reservoir prior to eruption. The internal high-An spikes may be produced by similar events earlier in the history of the Colima magma system that did not necessarily trigger eruption. The hydrothermal experiments indicate that plagioclase more calcic than An_{60} will not crystallize in the hybrid 1818 magma at 200 MPa or lower pressures. Although we did not find plagioclase with >An_{70} that can be related to the more mafic amphibole xenocrysts (G1), the most calcic plagioclase zones found close to the rims in the 1818 and 1913 magmas should represent the mixing events. Likewise, natural olivine was found only with resorbed margins and is thus though to be xenocrystic.

Additionally, experiments do not produce amphibole with Al contents as high as those observed in the G1 crystals (Fig. 6), so mixing is required to explain the presence of the G1 amphiboles. Almost all G1 amphiboles belong to the 1913 magma and only a few can be found in the 1818 magma. This suggests that the 1913 magma experienced large volume or more frequent injections of mafic magma that was partially mingled with the resident reservoir melt. One of those injections likely triggered the eruption, as seen in the thin TI rims and the lack of rims and dissolution textures in the 1913 G1 crystals. In contrast, the scarcity of G1 crystals in the 1818 magma, the abundance of G2 amphiboles with TI rims and the non-ubiquitous occurrence of crystals with TII rims suggest that the 1818 magma rather than been tapped as a

Table 3
Hydrothermal experiments on a 1818 Colima sample.

Experiment	Temperature (°C)	Pressure (MPa)	Experimental phase	Aliquote	Experiment type	Duration (h)
Col9	900	200	g,amph,ox,px	Natural sample	Waspaloy	240
Col10	850	200	g,plag,amph,ox,px	9	Waspaloy	168
Col11	900	100	g,plag,amph,ox,px	9	Waspaloy	168
Col12	850	100	g,plag,amph,ox,px	9	Waspaloy	168
Col15	900	150	g,amph,ox,px	9	Waspaloy	168
Col16	875	200	g,amph,ox,px	9	Waspaloy	168
Col20	875	200	g,amph,ox,px	12	Waspaloy	168
Col21	900	50	g,plag,ox,px	Natural sample	Waspaloy	240
Col22	975	150	g,amph,ox,px	Natural sample	TZM	240
Col24	800	200	g,plag,amph,ox,px	22	Waspaloy	168
Col25	875	100	g,plag,amph,ox,px	22	Waspaloy	168
Col26	825	200	g,plag,amph,ox,px	22	Waspaloy	168
Col27	950	100	g,ox,px	16	TZM	168
Col28	875	150	g,plag,amph,ox,px	22	Waspaloy	168
Col29	925	150	g,amph,ox,px	22	TZM	168
Col30	925	150	g,amph,ox,px	9	TZM	168
Col31	875	75	g,plag,ox,px	21	Waspaloy	168

g = groundmass glass, amph = amphibole, plag = plagioclase, ox = Fe-Ti oxide, px = pyroxene.
Mineral experimental phases represent new growth, euhedral crystals.

consequence of a singular event of mixing, it was continuously heated by more mafic magmas, but moderately mixed. Probably relatively small amounts of magma in the reservoir were raised to temperatures close to the amphibole and plagioclase stability field where amphiboles with TII rims resided for longer periods of time before eruption.

Although this scenario does not exclude the possibility that non-Plinian magmas erupt from the 1818–1913 reservoir (products erupted in the 1990–1999 period and the LHV and BSA prehistoric lavas where amphibole seems to were stable) it implies that frequent injections of more mafic magma dictates the dynamics of the 1818 and 1913 eruptions as seen at other volcanoes (e.g. Andrews et al., 2008; Sosa-Ceballos et al., 2014). In addition, it seems that magmas from the most recent eruptions are shallowly stored, as suggested by high-K dacitic melt inclusions in pyroxenes and plagioclase (Reubi et al., 2013). These magmas are amphibole-free, thus they could be stored as deeply as the 1818 magma, albeit at hotter conditions, or they could be stored shallowly where amphibole is not stable (<75 MPa at 900 °C). During the 1998–2005 period, decompression-crystallization was the main evolution process (Reubi et al., 2013). These processes are reflected in the more evolved composition of matrix groundmass compared to the melt inclusions (Fig. 8).

Indeed, it seems that explosive activity can be related to intermittent mixing processes at depth (≥200 MPa), where large amphiboles (hence, water-rich magmas) are incorporated into the ascending magma from deeper regions (Fig. 10). Although phlogopite xenocrysts from the K-rich magmas erupted in the surroundings and the recent Colima eruptions (Crummy et al., 2014) have never been reported for the 1818 and 1913 deposits, the variable alkaline composition of the mingled groundmass-glass for these deposits suggests that some alkaline mafic component could be replenishing the magma reservoir.

4.2. Building up a Plinian eruption?

During the last 15 years Volcán de Colima has become increasingly explosive (Saucedo et al., 2010), raising the question about the possibility of an eruption similar to those occurred in 1818 and 1913. The increase in amphibole has been related to explosive activity, and was suggested as a monitoring tool to forecast future explosive events

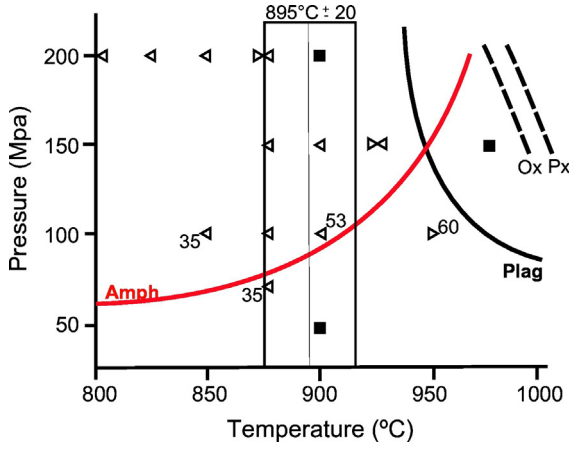

Fig. 7. Phase diagram for experiments on the 1818 magma. All experiments were water saturated ($P_{H2O} = P_{total}$) and run at an oxygen fugacity equal to NNO to NNO + 1. Glass (melt) and vapor are present at all conditions. Left pointing arrows represent crystallization experiments; right pointing arrows, melting experiments. Squares represent powders run directly at those conditions. Curves represent the upper stability limits for mineral phases (dashed curves were approximated). Temperature of 880 °C was calculated assuming equilibrium between An_{50} rims (most common in 1818 magma) and G2 amphiboles.

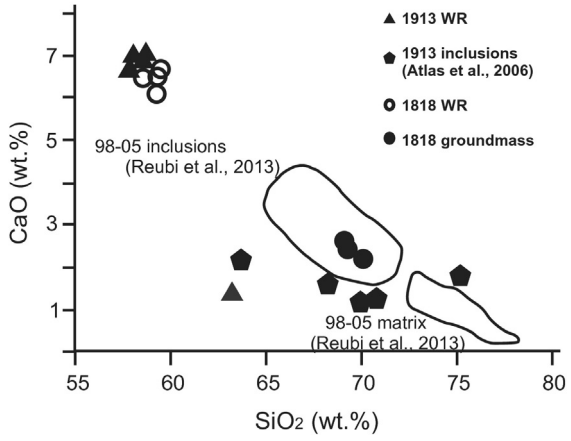

Fig. 8. Compositional variation of 1818 and 1913 pumice whole-rock (Saucedo et al., 2010), plagioclase melt inclusions (1913 only, Atlas et al., 2006). Groundmass-glass and melt inclusions from the 98–05 period (Reubi et al., 2013) and whole-rock compositions of the 1800–1913 period (Luhr and Carmichael, 1990a) are shown for comparison. Note how the whole rock of the 1913 pumice is less evolved than the plagioclase melt inclusions from the same deposit, which suggests either mixing with more mafic magmas just before eruption or resorption of phenocrysts due to a heating event.

Please cite this article as: Macías, J.L., et al., Storage conditions and magma processes triggering the 1818CE Plinian eruption of Volcán de Colima, J. Volcanol. Geotherm. Res. (2017), http://dx.doi.org/10.1016/j.jvolgeores.2017.02.025

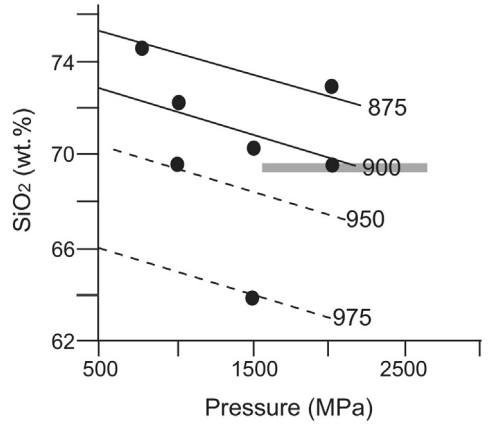

Fig. 9. SiO_2 of experimental glasses vs pressure. Isotherms of 875 and 900 °C are represented with solid lines. Isotherms for 950 and 975 °C are inferred with dashed lines. The colored box represents the pressure range (207 ± 52 MPa) at which the silica content of natural glass (69 wt%) intersects the average temperature calculated with amphibole and plagioclase (895 ± 20 °C).

(Luhr and Carmichael, 1990a, 1990b). We show that 1818 and 1913 Plinian deposits record an influx of mafic-amphibole (G1) into the system, whereas the effusive LHV and BSA prehistoric lavas contain amphibole, with thermal or decompression disequilibrium, but devoid of G1 type crystals, which coincides with this idea.

The Plinian magmas of 1818 and 1913 were stored and mixed with mafic pargasite-rich magmas at 170–210 MPa, whereas high-K melt inclusions in pyroxenes and plagioclase from the present-day eruption, amphibole-poor or amphibole-free, suggests shallow storage conditions (Reubi and Blundy, 2008; Atlas et al., 2006). The main difference between the 1818 and 1913 Plinian eruptions and the less explosive inter-Plinian eruptions could thus be the volume and frequency of intrusions of the pargasite-rich mafic magma, with G1 type crystals, into the Colima reservoir (Fig. 10).

How frequent a reservoir is replenished to erupt explosively is still debatable. Studies on Popocatépetl volcano found that plagioclase erupted during Plinian eruptions recorded at least 40 mixing events in one decade, although the volume of such injections is unknown (Sosa-Ceballos et al., 2014). One of these Plinian eruptions seems to be triggered by a single mixing event (Sosa-Ceballos et al., 2012); the volume of dense rock equivalent deposited is ~3 km^3, but the portion attributed to the mafic injected magma is practically impossible to quantify. Although, we can approximate by textural analysis of pumice, that <10% of the sample, belong to a more mafic groundmass, the amount of non-erupted mafic magma is still unknown. In summary, new approaches are needed in order to better quantify the amount of mixing needed to make a magma reservoir eruptible.

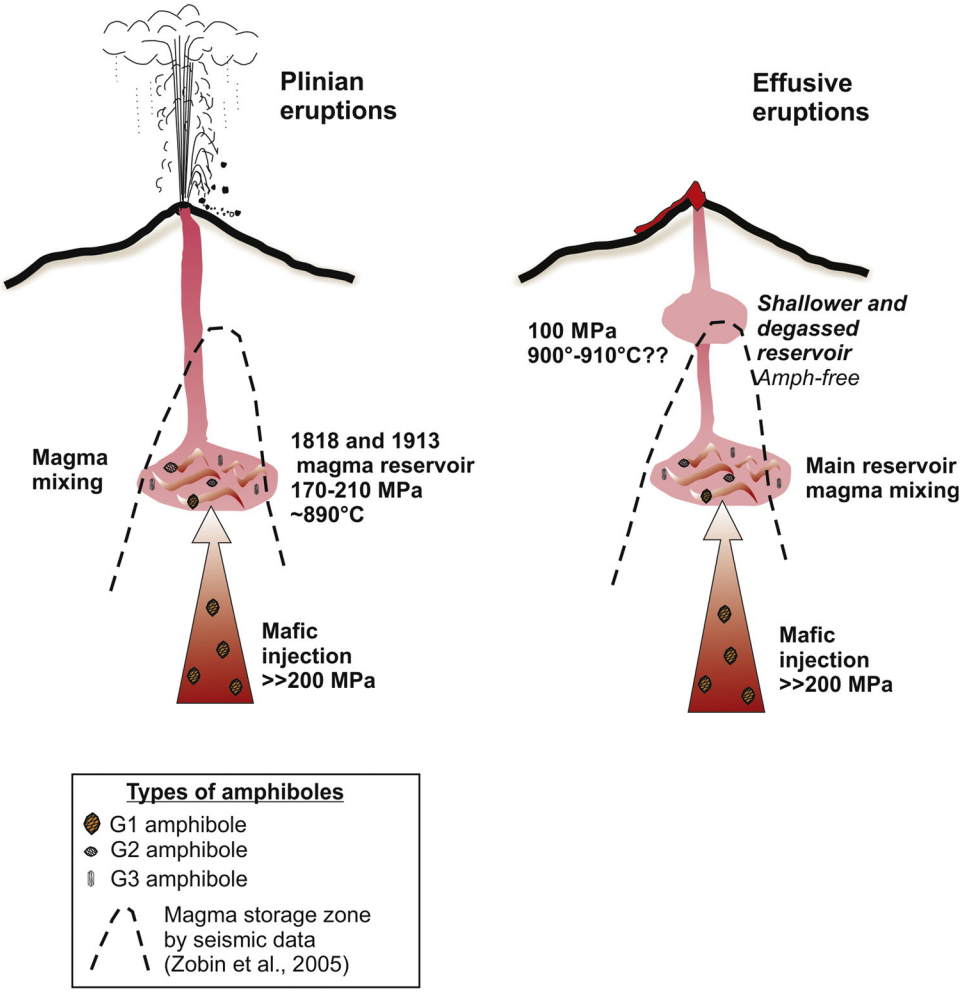

Fig. 10. Schematic model of the plumbing system of Volcán de Colima. The 1818 and 1913 magmas contain multiple evidence of mixing with more mafic magmas. Such mixing takes place at a reservoir where amphibole is stable (150–200 MPa). G1 amphiboles are injected into the Colima reservoir during mixing and are not related to assimilation of the local crust (Fig. 7). Contrary to Plinian magmas, effusive magmas lack frequent mixing events (scarce amphibole or lack of it). Their eruption could be from the deep reservoir (without the influence of mixing) or from shallow zones where amphibole is not stable.

Please cite this article as: Macías, J.L., et al., Storage conditions and magma processes triggering the 1818CE Plinian eruption of Volcán de Colima, J. Volcanol. Geotherm. Res. (2017), http://dx.doi.org/10.1016/j.jvolgeores.2017.02.025

Timing for mixing seems to be better constrained, recent studies have investigated the timescales of rim formation on amphiboles and its relation with eruption. De Angelis et al. (2015) demonstrates that amphibole reaction rims induced by heating experiments can grow quickly (3–48 h) and relatively thick (7–80 μm) when amphibole is heated to 50 °C out of equilibrium. Although the 1818 and 1913 matrix groundmass is not as silicic as the starting material used in this experimental work (75.9 wt% SiO_2), which would result in faster kinetics of rim growth, wider rims and bigger rim-crystals, the 10 μm rims on Colima amphiboles would record approximately 5 h of heating. Such timescale is surprising and would reflect how eruptable is a reservoir when is replenished with more mafic magmas. However, the sensitivity of amphibole to pressure, temperature and melt composition, and the kinetics of rim grow dominated by melt properties makes direct application of results from experimental studies challenging unless they are performed on the particular magma of interest.

In summary, if an influx of mafic magma is large enough, or there are sufficiently frequent smaller injections, and those magmas mix with the Colima magmas, then explosive eruptions will likely result. Recent seismicity analysis supports this idea. Ambient seismic noise suggest that the movement of magma from a deep reservoir (>15 km) into shallower zones would provoke deep seismicity below Volcán de Colima, which in fact, could indicate the possibility of large eruptions (Spica et al., 2016). If mafic melts cannot mix with the resident magmas or just pond and heat the reservoir, regardless of location in the plumbing system, then magmas can decompress more slowly, amphibole will have time to completely react, resulting in effusive eruption of magmas with few or no amphibole.

5. Conclusions

Phase equilibria and textural-compositional analysis of phenocrysts indicate that amphibole is stable in the 1818 Colima magma at 170–210 MPa and ~890 °C. Because the 1818 and 1913 eruptions have basically the same mineral association and they erupted magmas with similar composition (~58 wt% SiO_2), we infer that both magmas were stored at the same reservoir conditions. Although amphibole is stable in the 1818 and 1913 pumices, their abundance, textures and compositional variability indicate that mixing with more mafic magmas is a frequent process in the 1818–1913 magma reservoir. Regardless of their volume and frequency over time, the accumulation of these mixing events triggered the 1818 and 1913 Plinian eruptions. In contrast to the more explosive eruptions, the effusive emissions of lava are sourced from a more shallow region and do not contain amphibole added by magma mixing. Although more investigations about the shallow internal structure of the Colima volcanos are needed, we suggest that the mafic amphibole-rich magmas that replenished the 1818–1913 reservoir lack the ability to reach shallow depths within the Colima plumbing system.

Supplementary data to this article can be found online at http://dx.doi.org/10.1016/j.jvolgeores.2017.02.025.

Acknowledgments

This work was partially supported through grants from the Dirección General de Asuntos del Personal Académico, Universidad Nacional Autónoma de México (DGAPA-IN116911) to J.L.M., from National Science Foundation (EAR-0711043 and EAR-1049829) to J.E.G., and the Consejo Nacional de Ciencia y Tecnología (CONACYT-101548) to R.S.G. We want to thank Carlos Linares from the Laboratorio Universitario de Petrología (Geophysics Institute) and Noemí Salazar Hermenegildo (Micro Analysis Laboratory) for their assistance during microprobe analyses at UNAM. We are grateful with the ideas and comments that B. Andrews and M. Pichavant provide us to improve this contribution.

References

Allan, J., 1986. Geology of the Colima and Zacoalco grabens, SW Mexico: late Cenozoic rifting in the Mexican Volcanic Belt. Geol. Soc. Am. Bull. 97, 473–485.
Allan, J.F., Carmichael, I.S.E., 1984. Lamprophyric lavas in the Colima graben, SW Mexico. Contrib. Mineral. Petrol. 88, 203–216.
Andrews, B.J., Gardner, J.E., Housh, T.B., 2008. Repeated recharge, assimilation, and hybridization in magmas erupted from El Chichon as recorded by plagioclase and amphibole phenocrysts. J. Volcanol. Geotherm. Res. 175, 415–426.
Arreola, J.M., 1915. Catálogo de las erupciones antiguas del volcán de Colima. Mem. Rev. Soc. Cient. 32. Antonio Alzate, Mexico, pp. 443–481.
Atlas, Z.D., Dixon, J.E., Sen, G., Finny, M., Martin Del Pozzo, A.L., 2006. Melt inclusions from Volcán Popocatépetl and Volcán de Colima, Mexico: melt evolution due to vapor-saturated crystallization during ascent. J. Volcanol. Geotherm. Res. 153, 221–240.
Barcena, M., 1887. Informe sobre el estado actual del Estado de Colima. El Estado de Colima. Periódico Oficial del Gobierno. XXI, p. 2 (January).
Bonasia, R., Capra, L., Costa, A., Macedonio, G., Saucedo, R., 2011. Tephra fallout hazard assessment for a Plinian eruption scenario at Volcán de Colima (Mexico). J. Volcanol. Geotherm. Res. 203, 12–22.
Bretón, M., Ramírez, J.J., Navarro, C., 2002. Summary of the historical eruptive activity of Volcán de Colima, México: 1519–2000. J. Volcanol. Geotherm. Res. 117, 21–46.
Capra, L., Gavilanes-Ruíz, J.C., Bonasia, R., Saucedo, R., Sulpizio, R., 2014. Re-assessing volcanic hazard zonation of Volcán de Colima, México. Nat. Hazards 76, 41–61.
Capra, L., Macías, J.L., Cortés, A., Saucedo, R., Osorio-Ocampo, S., Dávila, N., Arce, J.L., Gavilanes-Ruíz, J.C., Corona-Chávez, P., García-Sánchez, L., Sosa-Ceballos, G., Vázquez, R., 2015. Preliminary report on the July 10–11, 2015 eruption at Volcán de Colima: pyroclastic density currents with exceptional runouts and volumes. J. Volcanol. Geotherm. Res. 310, 39–49.
Chertkoff, D.G., Gardner, J.E., 2004. Nature and timing of magma interactions before, during, and after the caldera-forming eruption of Volcán Ceboruco, Mexico. Contrib. Mineral. Petrol. 146, 715–735.
Coombs, M.L., Eichelberger, J.C., Rutherford, M.J., 2002. Experimental and textural constraints on mafic enclave formation in volcanic rocks. J. Volcanol. Geotherm. Res. 119, 125–144.
Cortés, A., Garduño-Monroy, V.H., Navarro-Ochoa, C., Komorowski, J.C., Saucedo, R., Macías, J.L., Gavilanes, J.C., 2005. Cartas Geológicas y Mineras 10. Carta Geológica del Complejo Volcánico de Colima, con Geología del Complejo Volcánico de Colima: México D.F., Universidad Nacional Autónoma de México, Instituto de Geología, escala 1:10,000, mapa con texto explicativo 37 p., 15 figs., 2 tablas.
Cortés, A., Garduño, V.H., Macías, J.L., Navarro, C., Komorowski, J.C., Saucedo, R., Gavilanes, J.C., 2010. Geological mapping of the Colima volcanic complex (Mexico) and implication for hazard assessment. Geol. Soc. Am. Spec. Pap. 464, 294-246.
Crummy, J.M., Savov, I.P., Navarro-Ochoa, C., Morgan, D.J., Wilson, M., 2014. High-K mafic Plinian eruptions of Volcán de Colima, Mexico. J. Petrol. 55, 2155–2192.
De Angelis, S.H., Larsen, J., Coombs, M., Dunn, A., Hayden, L., 2015. Amphibole reaction rims as a record of pre-eruptive magmatic heating: an experimental approach. Earth Planet. Sci. Lett. 426, 235–245.
De Angelis, S.H., Larsen, J., Coombs, M., 2013. Pre-eruptive magmatic conditions at Augustine volcano, Alaska, 2006: evidence from amphibole geochemistry and textures. J. Petrol. 54, 1939–1961.
De la Cruz-Reyna, S., 1993. Random patterns of occurrence of explosive eruptions at Colima Volcano, Mexico. J. Volcanol. Geotherm. Res. 55, 51–68.
Devine, J.D., Gardner, J.E., Brack, H.P., Layne, G.D., Rutherford, M.J., 1995. Comparison of microanalytical methods for estimation of H_2O contents of silicic volcanic glasses. Am. Mineral. 80, 319–328.
Gardner, J.E., Rutherford, M.J., Carey, S., Sigurdsson, H., 1995. Experimental constraints on preeruptive water contents and changing magma storage prior to explosive eruptions of Mount St. Hellens. Bull. Volcanol. 57, 1–17.
Garduño, V.H., Tibaldi, A., 1991. Kinematic evolution of the continental active triple junction of western Mexican Volcanic Belt. C.R. Acad. Sci. Paris. 312 pp. 135–142.
Geschwind, C.H., Rutherford, M.J., 1992. Cummingtonite and the evolution of the Mount St.Helens magma system: an experimental study. Geology 20, 1011–1014.
Holland, T., Blundy, J., 1994. Non-ideal interactions in calcic amphiboles and their bearing on amphibole-plagioclase thermometry. Contrib. Mineral. Petrol. 116, 433–447.
Komorowski, J.-C., Navarro, C., Cortés, A., Siebe, C., 1994. The repetitive collapsing nature of Colima volcanoes (México). Problems related to the distinction of multiple deposits and interpretation of ^{14}C ages with implications for future hazards. Universidad de Colima, Cuarta Reunión Internacional Volcán de Colima: A Decade Volcano Workshop, Colima, January 24–28. 1994, pp. 12–18.
Komorowski, J.C., Navarro, C., Cortés, A., Saucedo, R., Gavilanes, J.C., 1997. The Colima Volcanic Complex: Quaternary multiple debris avalanche deposits, historical pyroclastic sequences (pre-1913, 1991 and 1994). IAVCEI, Puerto Vallarta, México, 1997, Plenary Assembly, Excursión guidebook. Gobierno del Estado de Jalisco, Secretaria General, Unidad Editorial, Guadalajara, Jalisco, pp. 1–38.
Luhr, J.F., 1992. Slab-derived fluids and partial melting in subduction zones: insights from two contrasting Mexican volcanoes (Colima and Ceboruco). J. Volcanol. Geotherm. Res. 54, 1–18.
Luhr, J.F., 1997. Extensional tectonics and the diverse primitive volcanic rocks in the Western Mexican Volcanic Belt. Can. Mineral. 35, 473–500.
Luhr, J.F., 2002. Petrology and geochemistry of the 1991 and 1998–999 lava flows from Volcán de Colima, México: implications for the end of the current eruptive cycle. J. Volcanol. Geotherm. Res. 117, 169–194.
Luhr, J.F., Carmichael, I.S.E., 1980. The Colima volcanic complex México I. post-caldera andesites from Volcán Colima. Contrib. Mineral. Petrol. 71:343–372. http://dx.doi.org/10.1007/BF00374707.

Please cite this article as: Macías, J.L., et al., Storage conditions and magma processes triggering the 1818CE Plinian eruption of Volcán de Colima, J. Volcanol. Geotherm. Res. (2017), http://dx.doi.org/10.1016/j.jvolgeores.2017.02.025

Luhr, J.F., Carmichael, I.S.E., 1990a. Petrological monitoring of cyclic eruptive activity at Volcán Colima, México. J. Volcanol. Geotherm. Res. 42:235–260. http://dx.doi.org/10.1016/0377-0273(90)90002-W.

Luhr, J.F., Carmichael, I.S.E., 1990b. Geology of Volcán de Colima. Univ. Nac. Auton. México, Inst. Geol. Bol. 107 (101 pp.).

Luhr, J.F., Nelson, S.A., Allan, J.F., Carmichael, I.S.E., 1985. Active rifting in southwestern Mexico: manifestations of an incipient eastward spreading-ridge jump. Geology 13, 54–57.

Luhr, J.F., Prestegaard, K.L., 1988. Caldera formation at Volcan Colima, Mexico, by a large Holocene debris avalanche. J. Volcanol. Geotherm. Res. 35, 335–348.

Luhr, J.F., Navarro, C., Connor, C.B., Connor, L., 2006. The 1913 VEI-4 Plinian eruption of Volcán de Colima (Mexico): tephrochronology, petrology, and plume modelling: Eos, transactions, American Geophysical Union 87 (52), fall meeting supplementary. Dent. Abstr. V43B-1786.

Luhr, J.F., Navarro-Ochoa, C., Savov, I.P., 2010. Tephrochronology, petrology and geochemistry of late-Holocene pyroclastic deposits from Volcán de Colima, Mexico. J. Volcanol. Geotherm. Res. 197, 1–32.

Macías, J.L., Saucedo, R., Gavilanes, J.C., Varley, N., Velasco García, S., Bursik, M.I., Vargas Gutiérrez, V., Cortes, A., 2006. Flujos piroclásticos asociados a la actividad explosiva del volcán de Colima y perspectivas futuras. GEOS. 25(3), pp. 340–351.

Medina-Martínez, F., 1983. Analysis of the eruptive history of the Volcán Colima, México (1560–1980). Geofis. Int. 22, 157–178.

Mora, J.C., Macías, J.L., Saucedo, R., Orlando, A., Manetti, P., Vaselli, O., 2002. Petrology of the 1998–2000 products of Volcán de Colima, México. J. Volcanol. Geotherm. Res. 117:195–212. http://dx.doi.org/10.1016/S0377-0273(02)00244-5.

Mooser, F., 1961. Los Volcanes de Colima: Universidad Nacional Autónoma de México. Instituto de Geología. Bulletin 61, 49–71.

Navarro-Ochoa, C., Gavilanes-Ruíz, J.C., Cortés-Cortés, A., 2002. Movement and emplacement of lava flows at Volcán de Colima, México: November 1998–February 1999. J. Volcanol. Geotherm. Res. 117, 155–167.

Newhall, Christopher G., Self, Stephen, 1982. The volcanic explosivity index (VEI) an estimate of explosive magnitude for historical volcanism. J. Geophys. Res. Oceans 87 (C2), 1231–1238.

Pardo, M., Suarez, G., 1995. Shape of the subducted Rivera and Cocos plates in southern Mexico: seismic and tectonic implications. J. Geophys. Res. 100, 12357–12373.

Papale, P., Moretti, R., Barbato, D., 2006. The compositional dependence of the saturation surface of $H_2O + CO_2$ fluids in silicate melts. Chem. Geol. 229, 78–95.

Pichavant, M., Martel, C., Bourdier, J.-L., Scaillet, B., 2002. Physical conditions, structure, and dynamics of a zoned magma chamber: Mount Peleé (Martinique, Lesser Antilles Arc). J. Geophys. Res. 107 (B5). http://dx.doi.org/10.1029/2001JB000315.

Pichavant, M., Costa, F., Burgisser, A., Scaillet, B., Martel, C., Poussineau, S., 2007. Equilibration scales in silicic to intermediate magmas – implications for experimental studies. J. Petrol. 48, 1955–1972.

Reubi, O., Blundy, J., 2008. Assimilation of plutonic roots, formation of high-K exotic melt inclusions and genesis of andesitic magmas at Volcán de Colima, Mexico. J. Petrol. 49, 2221–2243.

Reubi, O., Blundy, J., Varley, N.R., 2013. Volatile contents, degassing and crystallization of intermediate magmas at Volcán de Colima, Mexico, inferred from melt inclusions. Contrib. Mineral. Petrol. 165, 1087–1106.

Robin, C., Mossand, P., Camus, G., Cantagrel, J.M., Gourgaud, A., Vincent, P., 1987. Eruptive history of the Colima Volcanic Complex (México). J. Volcanol. Geotherm. Res. 31, 99–113.

Robin, C., Komorowski, J.C., Boudal, C., Mossand, P., 1990. Evidence of magma mixing in juvenile fragments from pyroclastic surge deposits associated with debris avalanche deposits at Colima volcanoes, Mexico. Bull. Volcanol. 52, 391–403.

Robin, C., Camus, G., Gourgaud, A., 1991. Eruptive and magmatic cycles at Fuego de Colima volcano (Mexico). J. Volcanol. Geotherm. Res. 45, 209–225.

Roverato, M., Capra, L., Sulpizio, R., Norini, G., 2011. Stratigraphic reconstruction of two debris avalanche deposits at Colima Volcano (Mexico): insights into pre-failure conditions and climate influence. J. Volcanol. Geotherm. Res. 207, 33–46.

Roverato, M., Capra, L., 2014. Lacustrine sediments as result of an occasional volcanic lake by drainage natural damming and implication with paleoclimate (Colima volcano, Mexico). IAVCEI-5IMC Conference, Querétaro, Mexico, Abstract (3 pp.).

Rutherford, M.J., Devine, J.D., 2003. Magmatic conditions and magma ascent as indicated by hornblende phase equilibria and reactions in the 1995–2001 Soufriere Hills Magma. J. Petrol. 44, 1433–1454.

Savov, I.P., Luhr, J.F., Navarro-Ochoa, C., 2008. Petrology and geochemistry of lava and ash erupted from Volcán Colima, Mexico, during 1998–2005. J. Volcanol. Geotherm. Res. 174, 241–256.

Saucedo, R., Macías, J.L., 1999. La historia del Volcán de Colima: Tierra Adentro. 98 pp. 8–14.

Saucedo, G.R., Macías, J.L., Sheridan, M.F., Bursik, I., Komorowski, J.C., 2005. Modeling of pyroclastic flows of Colima Volcano, Mexico: implications for hazard assessment. J. Volcanol. Geotherm. Res. 139:103–115. http://dx.doi.org/10.106/j.jvolgeores.2004.06.019.

Saucedo, R., Macías, J.L., Gavilanes, J.C., Arce, J.L., Komorowski, J.C., Gardner, J.E., Valdez-Moreno, G., 2010. Eyewitness, stratigraphy, chemistry, and eruptive dynamics of the 1913 Plinian eruption of Volcán de Colima, México. J. Volcanol. Geotherm. Res. 191:149–166. http://dx.doi.org/10.1016/j.jvolgeores.2010.01.011.

Saucedo, R., et al., 2011. "Corrigendum to Eyewitness, stratigraphy, chemistry, and eruptive dynamics of the 1913 Plinian eruption of Volcan de Colima, Mexico" Journal of Volcanology and Geothermal Research 191 (2010) 149–166]. J. Volcanol. Geotherm. Res. 207 (1), 67.

Siebe, C., Rodríguez-Elizarrarás, S., Stoopes, G., Komorowski, J.C., Sheridan, M.F., 1992. How many debris avalanche deposits at the Colima volcanic complex or Quo Vadimus. abstract. Tercera Reunión Nacional Volcán de Colima y Segunda Reunión Internacional de Vulcanología. 15. Universidad de Colima, Colima (January 20–24).

Sisson, T.W., Grove, T.L., 1993. Experimental investigations of the role of H_2O in calk-alkaline differentiation and subduction zone magmatism. Contrib. Mineral. Petrol. 113, 143–166.

SOSA-CEBALLOS, Giovanni, et al., 2012. A caldera-forming eruption~ 14,100 14 Cyr BP at Popocatépetl volcano, México: Insights from eruption dynamics and magma mixing. J. Volcanol. Geotherm. Res. 213, 27–40.

Sosa-Ceballos, G., Gardner, J., Lassiter, J., 2014. Intermittent mixing processes occuring before Plinian eruptions of Popocatepetl volcano, Mexico: insights from textural-compositional variations in plagioclase and Sr-Nd-Pb isotopes. Contrib. Mineral. Petrol. 167, 966–985.

Spica, Z., Perton, M., Legrand, D., 2016. Anatomy of the Colima volcano magmatic system, Mexico. Earth Planet. Sci. Lett. http://dx.doi.org/10.1016/j.epsl.2016.11.010.

Valdez-Moreno, G., Schaaf, P., Macías, J.L., Kusakabe, M., 2006. New Sr-Nd-Pb-O isotope data for Colima volcano and evidence for the nature of the local basement. In: Siebe, C., Macías, J.L., Aguirre-Díaz, G.J. (Eds.), Neogene-Quaternary Continental Margin Volcanism: A perspective From Mexico: Geological Society of America Special Paper. 402, pp. 45–63.

Verma, S.P., Luhr, J.F., 1993. Sr-Nd-Pb isotope and trace element geochemistry of calc-alkaline andesites from Volcán de Colima, México. Geofis. Int. 32, 617–631.

Waitz, P., 1935. Datos históricos y bibliográficos acerca del Volcán de Colima. Mem. de la Soc. 53. Antonio Alzate, pp. 349–383.

Waters, L.E., Lange, R.A., 2015. An updated calibration of the plagioclase-liquid hygrometer-thermometer applicable to basalts through rhyolites. Am. Mineral. 100, 2172–2184.

Please cite this article as: Macías, J.L., et al., Storage conditions and magma processes triggering the 1818CE Plinian eruption of Volcán de Colima, J. Volcanol. Geotherm. Res. (2017), http://dx.doi.org/10.1016/j.jvolgeores.2017.02.025